

ANTIBACTERIAL AND PHYTOCHEMICAL PROPERTIES OF *ALCHORNEA CORDIFOLIA* FRACTIONS AGAINST UROPATHOGENS AND MOLECULAR DOCKING OF BIOACTIVE COMPOUNDS

Ekpiken Solomon Ekpiken* and Nneka Ndifon Agbiji

Department of Microbiology, University of Cross River State, Calabar, Nigeria.



*Corresponding Author: Ekpiken Solomon Ekpiken

Department of Microbiology, University of Cross River State, Calabar, Nigeria.

Article Received on 09/02/2025

Article Revised on 29/02/2025

Article Accepted on 19/03/2025

ABSTRACT

A. cordifolia has various pharmacological as well as therapeutic potentials. This present study was to determine antibacterial and phytochemical potentials of *A. cordifolia* fractions against uropathogens and molecular docking of bioactive compounds. Standard procedures were used in crude extraction and fractionation of the extract. Antibacterial susceptibility was performed using standard protocol. Spectroscopic analysis as well as molecular docking of the bioactive compounds were carried out following standard protocol; and 16S rRNA sequencing standard protocol was used to confirm the uropathogens previously isolated from urine. Antibacterial activities of the fractions revealed remarkable inhibitory activities against all the test bacterial isolates and were in the descending order: butanol > ethyl-acetate > dichloromethane > aqueous. The MIC index showed that butanol fraction is bactericidal. Gas Chromatography-Mass Spectroscopy results revealed the presence of fifteen (15) and thirteen (13) compounds for butanol and ethyl acetate fractions respectively. Major phytoconstituents identified include: eicosanoic acid, 4H-cyclopentacyclooctane, Ethyl iso-allochololate and Pregna-5,16-dien-20-one, 3-(acetyloxy)-16-methyl-, (3 β)- from butanol fraction and Pregna-5,16-dien-20-one, 3-(acetyloxy)-16-methyl-, (3 β)-, hexadecenoic acid, and 10-hydroxy, methyl ester from ethyl acetate. The drug-likeness and pharmacokinetic ADMET of the compounds indicated possible novel drugs for treatment of bacterial infections. These results are promising and point to the possible use of Pregna-5,16-dien-20-one, 3-(acetyloxy)-16-methyl-, (3 β) and Ethyl iso-allochololate as alternative sources of antibacterial agent.

KEYWORDS: ADMET, Molecular Docking, Uropathogens, *Alchornea cordifolia*, ligands, protein targets.**INTRODUCTION**

Alchornea cordifolia, a straggling shrub generally found along the coastal regions of West Africa belongs to the Euphorbiaceae family, and it is widely used in Africa, as a remedy for several illnesses (Effo *et al.*, 2013 and Sinan *et al.*, 2021). Its common name is “Christmas Bush” and it is called “Mbom” by the Ibibio and Efik tribes. Elsewhere in Nigeria, it is called “Banbani” in Hausa/Fulani, “Ipaesinyin” in Yoruba and “Ububo” in Igbo (Ebenyi *et al.*, 2017). The plant can grow up to 9.8 m tall in swampy areas (Ebenyi *et al.*, 2017). The leaf and stems of the plant are used traditionally as therapeutic agents to treat various kinds of diseases in Africa (Ebenyi *et al.*, 2017 and Djimeli *et al.*, 2017). Previous studies showed several pharmacological activities of *A. cordifolia* such as antimicrobial, (including antimalarial, and anti-diarrhoeal activities); anti-inflammatory, antioxidant and anti-diarrhoeal (Effo *et al.*, 2013; Djimeli *et al.*, 2017). *A. cordifolia* is traditionally used for the treatment of a number of bacterial (mostly urinary tract infection), fungal and

parasitic infections; and the leaf have been reported to be an effective wound healing agent (Asimole *et al.*, 2022).

Multidrug-resistance (MDR) is considered a global emergency because of its attendant treatment failure, high cost and mortality (Addis *et al.*, 2021). It is estimated that 700,000 people died annually worldwide due to drugs resistant pathogens, and by 2050 it is projected that 10 million lives annually and cumulatively 100 trillion of US dollars of economic output will be at risk due to rise of drug-resistant bacterial infection and reducing global GDP by up to 3.5% (Kourkouta *et al.*, 2017; Nyandjou, 2017). The emergence of strains harbouring extended-spectrum beta-lactamases (ES β Ls) is a global health challenge. Extended-spectrum beta-lactamases are group of enzymes, produced by Gram-negative bacteria that confer resistance to some of the world’s commonly prescribed antibiotics, including penicillin, aminoglycosides, first, second and third generation cephalosporins, etc. (Giwa *et al.*, 2018; Ahmed *et al.*, 2022 and Teferi *et al.*, 2023). The major

targets for antibiotics are structural proteins, or signalling molecules that are essential for bacterial survival such as cell wall, cell membrane genes, protein synthesis, folic acid metabolism, DNA and RNA synthesis (Singh *et al.*, 2021). Uropathogens have evolved various mechanisms of resistance such as target modification, efflux pump, escape from immune surveillance of host, and enzyme catalysed destruction to escape the effects of antimicrobial agents previously used in UTIs treatment and management (Yun *et al.*, 2014; Zhou *et al.*, 2015; Nain *et al.*, 2015 and Sharma *et al.*, 2016). This has led to the search for alternative treatment options from different sources, including medicinal plants (Chikowe *et al.*, 2024). Curative potentials of plants materials are well documented in many literatures, and are due particularly to the presence of pharmacologically important constituents (secondary metabolites) (Ilusanya *et al.*, 2012; Okagu *et al.*, 2018). Secondary metabolites found in medicinal plants possess arrays of pharmacological activities like antibacterial, antifungal, antioxidant, anticancer and anti-inflammation properties (Maduabuchi and Tobeckukwu, 2023; Okagu *et al.*, 2018).

Medicinal plants are screened for the presence of phytochemical compounds using analytical techniques such as Fourier Transform Infrared (FT-IR) and Gas Chromatography-Mass Spectrometry (GC-MS) (Okereke *et al.*, 2017). FT-IR and GC-MS methods have been respectively used in recent years to detect functional groups and identify a variety of bioactive therapeutic compounds present in medicinal plants (Okagu *et al.*, 2018). GC-MS is one of the most effective, rapid, and precise method for detecting a wide variety of chemicals, including alkaloids, esters, alcohols, organic acids, steroids, long-chain hydrocarbons and amino acids using small amount of plant extracts. The unknown organic compounds in a complex mixture can be determined by the interpretation and also by matching the spectra with the database (Maduabuchi and Tobeckukwu, 2023).

Computer based approaches have emerged as advanced techniques that can be used to screen bioactive compounds derived from medicinal plants for drugs discovery. Computational prediction models (predictive tools) are crucial in guiding the methodology selection process for pharmaceutical and technology research. They have also been used in *in silico* forecast of pharmacokinetic, pharmacological and toxicological performance (Mir *et al.*, 2022). At Present, molecular docking is an efficient and cost-effective approach for developing and testing pharmaceuticals. This approach investigates numerous attaching mechanisms of actions against a specific biological receptor (usually protein) in order to evaluate the most effective interaction mechanism (Chaudhary and Tyagi, 2024). Furthermore, this technique facilitates systemic investigation by non-covalently placing a molecule into the binding site of an object macromolecule, resulting in specific binding at the active sites of every ligand (Chaudhary and Tyagi, 2024;

Chikowe *et al.*, 2024). Therefore, the current study was conducted to evaluate the antibacterial and phytochemical properties of *A. cordifolia* fractions against uropathogens and *in-silico* analysis for the most abundant compounds against some target proteins.

Taxonomical classification of *A. cordifolia*

Kingdom: Plantae
Division: Tracheophyta
Class: Magnoliopsida
Order: Malpighiales
Family: Euphorbiaceae
Genus: *Alchornea*
Species: *A. cordifolia*.

MATERIALS AND METHODS

Collection and authentication of plant materials

Fresh leaves of *A. cordifolia* were obtained from the botanic farm, Department of Pharmacognosy and Natural Medicine, Faculty of Pharmacy, University of Uyo, Uyo, Akwa Ibom State, Nigeria. The plant was identified and authenticated by a plant taxonomist in the Department of Pharmacognosy and Natural Medicine, Faculty of Pharmacy, University of Uyo, Uyo and the specimen deposited in the herbarium unit of the Department and a voucher number UUPH 31(b) allocated.

Phenotypic identification of bacterial stains

The test uropathogens used in this study were stock cultures of *Bacillus thuringiensis*, *Staphylococcus aureus*, *Proteus mirabilis*, *Klebsiella pneumoniae*, *Escherichia coli*, *Enterobacter cloacae* and *E. aerogenes* previously obtained from urine specimen of urinary tract infection patients (Ekpiken *et al.*, 2024). The stock bacterial cultures were sub-cultured into nutrient agar medium and grown for 18-24 h at 37 °C until visible colonies emerged on the plate. The bacterial strains were maintained in nutrient agar slant for molecular identification.

Molecular characterisation and identification of bacterial isolates

The maintained nutrient agar slant was grown on nutrient agar plates and a single visible colony was inoculated into sterile tryptic soy broth for DNA extraction. The cultures were grown overnight and centrifuged at 5,000 rpm for 5 min at room temperature and the cell pellet was washed with Tris buffer (10 mM Tris-HCl, 1 mM EDTA and 0.1 M NaCl, pH 8.0) and treated with lysozyme and RNase at 37 °C. The suspension was further treated with 15 µL of 20% sodium dodecyl sulphate (SDS) at 65 °C for 30 min and 3 µL of proteinase K at 65 °C at 2 h. The mixture was mixed with NaCl and the supernatant was collected after centrifugation. An equal amount of alcohol was added to the supernatant to precipitate DNA. The DNA was suspended in Tris-EDTA buffer after washing with 70% alcohol, air-dried at room temperature for approximately 3 h (Kaur *et al.*, 2020). The 16S rRNA sequence of the bacterial isolates was amplified using universal primers:

27F (5'-AGAGTTTGATCCTGGCTCAG-3') and 1525R (5'-AAGGAGGTGATCCAGCC-3'). The PCR reaction mix (66.3 μ L) was composed of 10 μ L of 5XGo Taq buffer, 3 μ L of 25 mM MgCl₂, 1 μ L of 10 mM dNTPs mix, 42 μ L of molecular grade water, 1 μ L each of the forward and reverse primers, 8 μ L of DNA template and 1.3 μ L of Taq DNA polymerase (Kaur *et al.*, 2020; Akbar *et al.*, 2022). The PCR was performed in a thermocycler (Applied Biosystem Inc., USA). The PCR-amplified product was purified using a PCR or Gel extraction kit following manufacturer's guide. The purified PCR products of 16S rRNA were sequenced following Sanger method (França *et al.*, 2002) using a Genetic Analyzer 3130xl sequencer (Applied Biosystem Inc., USA). The sequences obtained were used for gene similarity search against the National Centre for Biotechnology Information (NCBI) database using Basic Local Alignment Search Tool (BLAST) algorithm. The 16S rRNA sequences of all the isolates were submitted in the NCBI GenBank database (<https://www.ncbi.nlm.nih.gov/search/all/?term=>) and accession numbers obtained.

Plant extraction and fractionation of extract

The leaves of the plant were washed thoroughly with running tap water, shade dried at room temperature (25-30 °C) for 2 weeks, and pulverized using laboratory mortar and pestle. The coarse particles were further reduced to fine power using electric blender. *A. cordifolia* leaf (200.0 g) was macerated with 2.0 L of 70% ethanol at room temperature for 72 h with occasional agitation at interval. The extract was concentrated by evaporation using a water bath at 60 °C, and then stored at 4 °C for future purposes. Exactly 50.0 g of the extract was dissolved in 500.0 mL of distilled water and partitioned successively and exhaustively with ethyl acetate, dichloromethane (DCM) and *n*-butanol using a separating funnel (1,000.0 mL) capacity to obtain their respective fractions (Abubakar and Haque, 2020). The fractions were concentrated *in vacuo* at 35 °C to dryness.

Antibacterial activity of fractions of *A. cordifolia* leaf ethanol extract

Agar well diffusion method was used to determine the antibacterial activities of the various fractions of *A. cordifolia* leaves ethanol extract according to the method adopted by Gonelimali *et al.* (2018). About 0.1 mL of the standardized bacterial suspension was spread on the surface of dry Mueller-Hinton agar plates and allowed to seed. A sterile 6 mm cork borer was used to bore five equidistant wells on the seeded agar plates, while the sixth well was used for negative control (10% DMSO). About 0.1 mL of the various concentrations of the fractions (500, 250, 125, 62.5 and 31.25 mg/mL) was transferred into the wells. The seeded plates were left at room temperature for 15 min to allow for proper diffusion of the fractions into the agar plates and thereafter incubated at 37 °C for 24 h. The antibacterial assay was performed in duplicate. Antibacterial assay of

the fractions was determined by measuring the diameter of zone of inhibition to the nearest millimeter with a ruler. The measured diameter of zone of inhibition was interpreted according to (Udoh *et al.*, 2019). The inhibition zone values ≥ 13 mm = sensitive, 10-12 mm = moderately sensitive and ≤ 10 mm = Resistant. The minimum inhibitory concentration (MIC) and minimum bactericidal concentration (MBC) values for the extract were also determined.

Mechanism of antibiosis of butanol fraction of *A. cordifolia* leaf ethanol extract

The mechanism of antibiosis of the extracts was calculated using the MIC index ratio as described by Mogana *et al.* (2020) to determine whether the observed antibacterial activities were static or cidal. MIC index ratio ≤ 4 , was considered as bactericidal effect and MIC ratio > 4 , was considered as bacteriostatic effect.

Gas Chromatography Mass Spectroscopy (GC-MS) analysis

The GC-MS analysis of *A. cordifolia* fractions was done using methods described by Dandekar *et al.* (2015). The extract was dissolved in methanol and the inert gas, helium was used as carrier gas with the flow rate of 1 mL/min. HP5 column with specification length of 30 mm, internal diameter 0.32 mm, film of 0.25 mm and temperature limit -60 °C to 325 °C (350 °C) was used. The total run time of GC was 35 minutes. The oven temperature was raised from 70 °C up to 280 °C with the rate of 8 °C per minute rise in temperature. Exactly 4.0 μ L of the sample was injected through the injector. The MS was taken at 70eV. The identification of compounds was done by comparing the spectrum of unknown compounds with the spectrum of known compounds available in the computer library of National Institute of Standard and Technology (NIST MS 2.0) and the name, molecular weight, molecular formula and structure determined.

Molecular docking simulation

Ligands and Targets Preparation

The ligands identified using GC-MS and target proteins used in this study were downloaded from the PubChem (<https://www.pubchem.ncbi.nlm.nih.gov>) and RCSB (<https://www.rcsb.org>) databases in SDF and PDB formats respectively. The protein targets were prepared using the Biovia Discovery Studio software by eliminating water molecules from the structures, identifying the active binding sites and addition of hydrogen molecules to the protein structures. Similarly, the ligands were created and designed using ChemSketch software tool (www.acdlabs.com) (Dahiru *et al.*, 2024).

Molecular docking

The molecular docking protocol was carried out using the AutoDock Vina wizard to determine the binding affinity with exhaustiveness value set to 15. The ligand-target docked complexes were save in PDB and

visualized in 2D and 3D conformation using BioVia Discovery Studio visualizer (Dahiru *et al.*, 2024).

ADMET prediction and drug likeliness

The pharmacokinetics parameters (ADMET) (absorption, distribution, metabolism, excretion, and toxicity) of the ligands were predicted using SWISS ADME (www.swissadme.ch/) online tool to determine their drug likeliness and medicinal chemistry (Daina *et al.*, 2017).

RESULTS

Molecular characterisation and identification of bacterial isolates The results of the molecular characterisation and identification of isolated bacterial isolates based on 16S rRNA conserved gene sequences using universal primers is presented in Table 1. The result represents the NCBI

BLAST result of the bacterial isolates showing the accession number, % similarity, E value and query cover. Seven bacterial isolates comprising five Gram- negative bacteria and two Gram-positive bacteria were identified using National Centre for Biotechnology Information (NCBI). The gene sequences were deposited in the GenBank database and accession numbers of the bacterial isolates obtained. Figure 1 shows the gel electrophoresis of the amplified bacterial DNA conserved region. The result showed that the bacterial DNA from the isolates aligned along 1,500 bp DNA molecular weight ladder. This indicates that the isolated bacterial DNA were seemingly identical and the sequence percentage similarity ranged from 99.84% to 100%.

Table 1: NCBI BLAST Showing the Identity of the Bacterial Isolates.

Sample ID	Scientific Name	Max Score	Total Score	Query Cover	E value	% Ident.	Accession No.
GHU-01	<i>Bacillus thuringiensis</i>	1884	1884	100%	0	100.00	OR605730
GMU-07	<i>Proteus mirabilis</i>	2250	15558	100%	0	100.00	OR605733
GHU-09	<i>Enterobacter cloacae</i>	2575	2575	100%	0	100.00	OR605737
GMU-12	<i>Enterobacter aerogenes</i>	2250	2250	100%	0	99.92	OR605738
GHU-010	<i>Staphylococcus aureus</i>	2290	2290	99%	0	99.84	OR875985
GHU-05	<i>Escherichia coli</i>	2266	2266	99%	0	99.84	OR875986
GHU-06	<i>Klebsiella pneumoniae</i>	2283	2283	99%	0	100.00	OR875987

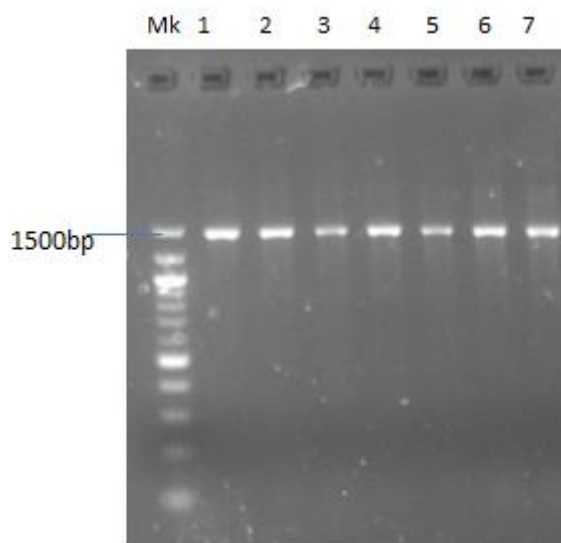


Figure 11: Agarose Gel electrophoresisogram showing the positive amplification of the 16S rRNA partial amplicon from the selected bacterial isolates. Lane 1= *P. mirabilis*, Lane 2= *E. aerogenes*, Lane 3= *E. cloacae*, Lane 4= *S. aureus*, Lane 5 = *E. coli*, Lane 6= *K. pneumoniae*, Lane 7= *B. thuringiensis*.

Antibacterial assay of fraction of *A. cordifolia* leaf ethanol extract

Antibacterial activity spectra of fractions of *A. cordifolia* leaf ethanol extract is presented in Table 26. *n*-Hexane fraction showed small zones of inhibitions against *E. aerogenes* 2, *B. thuringiensis* and *S. aureus*, which has inhibition zones less than 12.0±0.0 mm at 500 mg/mL and other bacterial isolates showed no resistance having with no inhibition zone. Observably, dichloromethane

fraction showed better activity than *n*-hexane fraction as it showed varying degrees of inhibitory zones against all the isolates at 500 and 250 mg/mL ranging from 11.0±1.0 to 19.0±1.0 mm. *P. mirabilis* and *E. aerogenes* were also susceptible to the fraction at 125 mg/mL, however, the least concentration showed no inhibition effect against the bacterial isolates Conversely, butanol fraction showed remarkable large inhibition zones against the test bacterial isolates at 500 mg/mL to 62.5

mg/mL, ranging from 10.0±2.0 to 26.0±1.0 mm, however, *E. cloacae*, *K. pneumoniae* and *S. aureus* and did not show activity at 31.25 mg/mL but smaller zones of inhibition were observed in *P. mirabilis*, *E. aerogenes*, *B. thuringiensis* and *E. coli*. Ethyl acetate fraction showed inhibitory zones against all bacterial isolates up to 125 mg/mL, however, antibacterial activity against *K. pneumoniae* was observed up to the least concentration; and against *S. aureus* and *B. thuringiensis*, activity was also observed up to 62.5 mg/mL. Aqueous fraction showed smaller inhibition zone against *P. mirabilis* at 500 mg/mL and large inhibition zones against *E. coli* at 500 mg/mL and 250 mg/mL.

The MIC and MBC of butanol fraction of *A. cordifolia* leaf against the test bacteria is presented in Table 3. The MIC ranged between 31.25 mg/mL and 125 mg/mL against all the test bacterial isolates, and the least was observed in Gram negative bacteria. The MBC ranged from 62.5 mg/mL to 125 mg/mL for all bacterial isolates, and the MIC indices ranged between 1.0 to 4.0, indicating a bactericidal agent.

GC-MS identification of compounds in *A. cordifolia* fractions

The GC-MS results of butanol and ethyl acetate fractions of *A. cordifolia* leaf ethanol extract revealed the presence

of fifteen (15) and thirteen (13) phytochemical compounds respectively. The identities of the bioactive compounds were confirmed based on the peak area and retention time (Table 4 and Table 5). The GC-MS chromatogram of the butanol and ethyl acetate fractions of *A. cordifolia* leaf ethanol extract is shown in Figure 2. The major phytoconstituents in the butanol fraction were Eicosanoic acid (20.93%), 4H-Cyclopentacycloctene, decahydro- (16.74%), Benzene, (2-ethyl-4-methyl-1,3-pentadienyl)-, (E)- (11.26%), Octadecanoic acid (9.78%), 1,4-Methanoazulene-9-methanol, decahydro-4,8,8-trimethyl-, [1S-(1α,3αβ,4α,8αβ,9R*)]- (9.28%), Pregna-5,16-dien-20-one, 3-(acetyloxy)-16-methyl-, (3β)- (6.52%) Ethyl iso-allocholate (5.23%), Docosanoic acid, 1,2,3-propanetriyl ester (4.03%), Linoleic acid ethyl ester (3.39%), Octacosanol (3.65%), Hexadecanoic acid, 1,1-dimethylethyl ester (2.32%). Similarly, the major phytoconstituents in the ethyl acetate fraction were Pregna-5,16-dien-20-one,3-(acetyloxy)-16-methyl-, (3β)- (37.79%), Hexadecanoic acid, 10-hydroxy-, methyl ester (14.21%), Oleic acid (9.70%), 1,4-Eicosadiene (7.52%), 7-Tetracyclo [6.2.1.0(3.8)0(3.9)] undecanol (5.80%), γ-Sitosterol, 9,12-Octadecadienoic acid (4.22%) each. The molecular structures of eight (8) major phytoconstituents identified in the butanol and ethyl acetate fractions of *A. cordifolia* leaf ethanol extract is presented in Figure 2.

Table 2: Antibacterial activities of fractions of *A. cordifolia* leaf ethanol extract against bacterial isolates.

Test Isolates	Concentrations of fractions (mg/mL) and mean zone of inhibitions (mm)									
	Ethyl acetate					Aqueous				
	31.25	62.5	125	250	500	31.25	62.5	125	250	500
<i>E. cloacae</i>	NZI	NZI	9.0±1.0	13.0±0.0	15.0±0.0	NZI	NZI	NZI	NZI	NZI
<i>P. mirabilis</i>	NZI	NZI	11.0±0.0	14.0±1.0	18.0±0.0	NZI	NZI	NZI	NZI	11.0±0.0
<i>E. aerogenes</i>	NZI	NZI	11.0±1.0	15.0±1.0	19.5±1.5	NZI	NZI	NZI	NZI	NZI
<i>B. thuringiensis</i>	NZI	12.5±0.5	15.0±0.0	20.0±1.0	24.0±1.0	NZI	NZI	NZI	NZI	NZI
<i>E. coli</i>	NZI	NZI	10.0±0.0	13.0±0.0	16.0±1.0	NZI	NZI	NZI	12.0±1.0	16.0±1.0
<i>K. pneumoniae</i>	11.0±1.0	13.0±1.0	16.0±1.0	21.0±1.0	25.0±1.0	NZI	NZI	NZI	NZI	NZI
<i>S. aureus</i>	NZI	10.0±1.0	13.0±1.0	16.0±1.0	22.0±1.0	NZI	NZI	NZI	NZI	NZI

Table 2: Cont'd: Antibacterial activities of fractions of *A. cordifolia* leaf ethanol extract against bacterial isolates.

Test Isolates	Concentrations of fractions (mg/mL) and mean zone of inhibitions (mm)									
	DCM					Butanol				
	31.25	62.5	125	250	500	31.25	62.5	125	250	500
<i>E. cloacae</i>	NZI	NZI	NZI	11.0±0.0	15.5±0.5	NZI	10.0±2.0	10.0±1.0	14.0±1.0	20.5±0.5
<i>P. mirabilis</i>	NZI	9.0±0.0	12.0±2.0	15.0±1.0	19.0±1.0	9.0±1.0	12.5±1.5	15.5±0.5	20.0±0.0	24.0±1.0
<i>E. aerogenes</i>	NZI	10.0±0.0	11.0±1.0	13.5±.05	15.0±0.0	11.5±1.5	12.0±1.0	14.0±0.0	16.0±1.0	25.0±0.0
<i>B. thuringiensis</i>	NZI	NZI	NZI	11.5±0.5	13.5±1.5	9.0±1.0	10.5±1.5	10.0±0.0	12.5±0.5	15.5±0.5
<i>K. pneumoniae</i>	NZI	NZI	NZI	14.5±0.5	16.5±0.5	NZI	13.0±1.0	15.0±1.0	22.0±1.0	26.0±1.0
<i>S. aureus</i>	NZI	NZI	NZI	14.0±0.0	17.5±0.5	NZI	9.0±1.0	11.0±1.0	14.0±1.0	16.0±1.0
<i>E. coli</i>	NZI	NZI	NZI	14.5±0.5	15.5±0.5	12.0±1.0	14.0±0.0	16.0±1.0	17.0±1.0	20.0±1.0

Table 3: MIC, MBC and MIC index values of butanol fraction of *A. cordifolia* ethanol leave extract against test bacterial isolates.

Test Isolates	Concentrations (mg/mL)		
	<i>cordifolia</i> butanol fraction		
	MIC	MBC	MIC INDEX
<i>K. pneumoniae</i>	31.25	62.5	2.0
<i>E. coli</i>	31.25	62.5	2.0

<i>S. aureus</i>	62.5	62.5	1.0
<i>E. aerogenes</i>	31.25	125	4.0
<i>E. cloacae</i>	62.5	62.5	1.0
<i>P. mirabilis</i>	125	125	1.0
<i>B. thuringiensis</i>	125	125	1.0

Table 4: Bioactive compounds identified from butanol fraction of *A. cordifolia* leaf by GC-MS.

Peak	R. Time (min)	Area %	Name of Compounds	Molecular Formular
1	5.435	1.997	Tridecane	C ₁₃ H ₂₈
2	5.543	1.580	cis-7-Tetradecen-1-ol	C ₁₄ H ₂₈ O
3	6.224	2.315	Hexadecanoic acid, 1,1-dimethylethyl ester	C ₂₀ H ₄₀ O ₂
4	6.379	1.724	9,12-Octadecadienoic acid (Z,Z)-	C ₁₈ H ₃₂ O ₂
5	6.819	11.258	Benzene, (2-ethyl-4-methyl-1,3-pentadienyl)-, (E)-	C ₁₄ H ₁₈
6	6.871	6.519	Pregna-5,16-dien-20-one, 3-(acetyloxy)-16-methyl-, (3β)-	C ₂₄ H ₃₄ O ₃
7	6.922	9.778	Octadecanoic acid	C ₁₈ H ₃₆ O ₂
8	7.020	3.645	Octacosanol	C ₂₈ H ₅₈ O
9	7.077	1.577	γ-Sitosterol	C ₂₉ H ₅₀ O
10	7.151	20.934	Eicosanoic acid	C ₂₀ H ₄₀ O ₂
11	7.455	3.398	Linoleic acid ethyl ester	C ₂₀ H ₃₆ O ₂
12	7.500	9.278	1,4-Methanoazulene-9-methanol, decahydro-4,8,8-trimethyl-, [1S-(1α,3αβ,4α,8αβ,9R*)]-	C ₁₅ H ₂₆ O
13	7.592	16.735	4H-Cyclopentacyclooctene, decahydro-	C ₁₁ H ₂₀
14	7.643	5.233	Ethyl iso-allocholate	C ₂₆ H ₄₄ O ₅
15	10.922	4.030	Docosanoic acid, 1,2,3-propanetriyl ester	C ₆₉ H ₁₃₄ O ₆

Table 5: Bioactive compounds identified from ethyl acetate fraction of *A. cordifolia* leaf by GC-MS.

Peak	R. Time (min)	Area %	Name of Compounds	Molecular Formular
1	3.655	2.534	Ethylbenzene	C ₈ H ₁₀
2	4.491	2.608	Hexanoic acid	C ₆ H ₁₂ O ₂
3	5.435	1.851	Octadecanoic acid	C ₁₈ H ₃₆ O ₂
4	6.814	14.206	Hexadecanoic acid, 10-hydroxy-, methyl ester	C ₁₇ H ₃₄ O ₃
5	6.871	4.220	9,12-Octadecadienoic acid	C ₂₈ H ₄₂ O ₄
6	6.917	7.522	1,4-Eicosadiene	C ₂₀ H ₃₈
7	7.014	3.491	1.2-cis-9-Octadecenyloxyethano	
8	7.100	3.273	Pentadecanoic acid	C ₁₇ H ₃₄ O ₂
9	7.495	37.799	Pregna-5,16-dien-20-one,3-(acetyloxy)-16-methyl-, (3β)-	C ₂₄ H ₃₄ O ₃
10	7.580	4.220	γ-Sitosterol	C ₂₉ H ₅₀ O
11	8.336	2.780	1,4-Methanoazulen-7(1H)-one	C ₁₅ H ₂₄ O
12	9.034	5.801	7-Tetracyclo[6.2.1.0(3.8)0(3.9)]undecanol	C ₁₅ H ₂₄ O
13	10.911	9.703	Oleic acid	C ₃₉ H ₇₆ O ₃

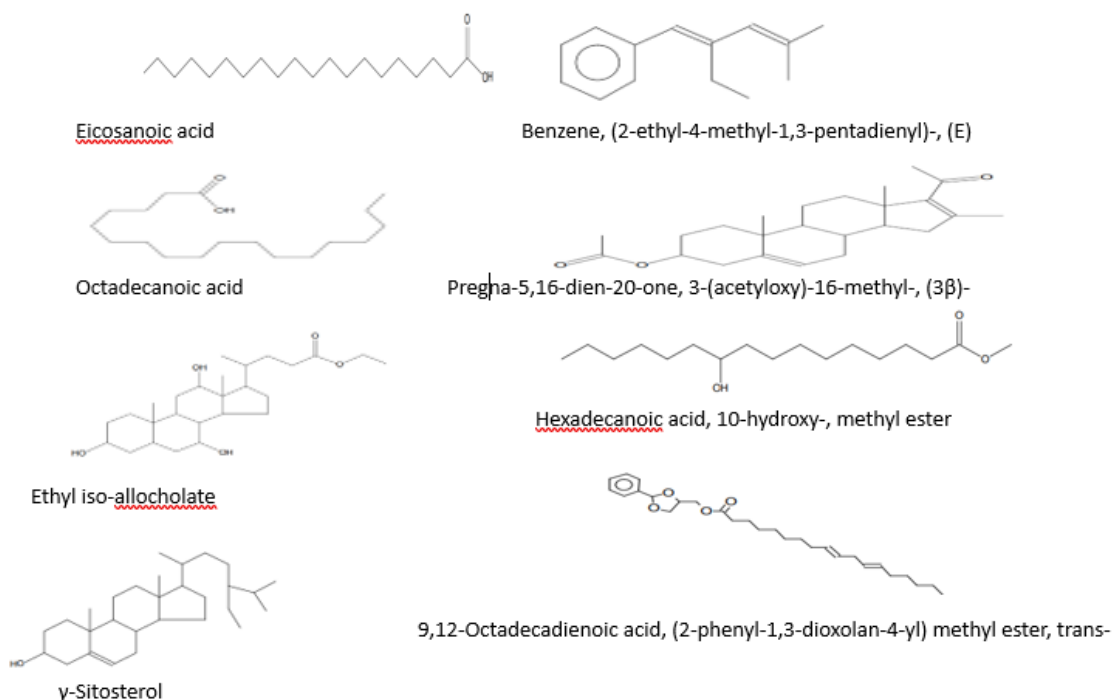


Fig. 2: Structures of major phytochemical constituents identified in the butanol and ethyl acetate fraction of *A. cordifolia* leaf ethanol extract using Gas Chromatography-Mass Spectrometry (GC-MS).

Selection of Ligands and Protein Targets

The list of the ligands and protein targets are presented in Table 6 and Table 7 including their PubChem ID and PDB ID respectively. The ligands were selected from the GC-MS results for the docking analysis. The standard drug (ciprofloxacin) was downloaded from drugBank database (www.go.drugbank.com/drugs). The detailed molecular docking results, amino acid residues, bond length and binding affinity are presented in Table 8 and Figure 3. From the docking results, the ligands were observed to show better affinity to the protein targets, except 6HIX that showed equal binding affinity with the standard drugs. Also, the molecular interactions involved in the selected complexes and the amino acids present is presented in Table 9. The results revealed formation of bond and non-bond interactions predominantly made up of hydrogen bond and alkyl bond. Other bonds formed include: carbon-hydrogen (C-H) bond, pi-alkyl bond, pi-anion bond, pi-sigma and, amide-pi stacked and halo-bond.

The results of drug-likeness parameters of the ligands are presented in Table 10, and SwissADME online tool was used to predict *in silico* drug-likeness parameters and ADMET features of the ligands. The ligands were predicted to be moderately soluble with high gastrointestinal absorption level. Moreover, the ligands have a lipophilicity, water solubility and skin permeation values of PAM (4.11 Log $P_{o/w}$, -4.64 Log S and -5.14 cm/s) and EIA (2.18 Log $P_{o/w}$, -3.84 Log S and -6.37 cm/s), which is within the acceptable limit. Furthermore, PAM is blood brain barrier (BBB) permeable while EIA is not. Also, the oral bioavailability of the ligands is within the acceptable limit. Moreover, all drug-likeness rules (Lipinski, Ghose, Veber, Muegge and Egan) of the ligands were with no violation. Although, no PAINS alert was predicted, however, there was one lead-likeness violation in the ligands. Synthetic accessibility score of 5.17 and 4.91 was observed for PAM and EIA.

Table 6: List of Ligands.

Ligands	PubChem ID
Pregna-5,16-dien-20-one,3-(acetyloxy)-16-methyl-, (3β)- (PAM)	7091834
Ethyl iso-allochololate (EIA)	6452096
Ciprofloxacin (CPX) (Standard)	DB00537

Table 7: List of Protein Targets.

Protein Targets	PDB ID	Microbial Source	Reference
Dihydrofolate reductase	1RG7	<i>E. coli</i>	Sawaya and Kraut 1997
Penicillin-binding protein	704C	<i>S. aureus</i>	Martinez-Caballero <i>et al.</i> , 2023
AcrB multidrug efflux pump	8FFK	<i>K. pneumoniae</i>	Zhang <i>et al.</i> , 2023
Structural protein	4ASS	<i>B. thuringiensis</i>	Hartley and Bennett, 2009

Cell adhesion	6HIX	<i>P. mirabilis</i>	Jiang <i>et al.</i> , 2018
Lipid transport	6MIT	<i>E. cloacae</i>	Owens <i>et al.</i> , 2019

Table 8: Molecular docking interactions between 6 different proteins (4ASS, 6HIX, 6MIT) with 4 ligands (Ciprofloxacin, EIA and PAM) and 3 proteins (1RG7, 7O4C and 8FFK) with 2 ligands (Ciprofloxacin and PAM).

Interaction	Amino acid residue	Bond length (Å)	Binding affinity (kcal/mol)
4ASS+PAM	ASN G:42, SER G:78, SER F:78	1.84, 2.87, 3.06	-7.2
4ASS+EIA	PHE H:58, LYS H:54, PRO H:55, SER G:53	4.97, 4.90, 5.21, 4.20, 3.32	-7.8
4ASS+CPX	ASP G:21, ASN H:62, LEU G:52, DT Y:16, PRO H:55	3.37, 5.18, 2.11, 4.54, 2.57, 3.27, 4.60	-7.1
6HIX+PAM	ALA A:47, HIS A:214, ILE A:42	4.31, 5.41, 3.65, 2.39, 5.39	-5.2
6HIX+EIA	ILE A:42, ALA A:47, ARG A:52, HIS A:214, TYR A:50, ASN A:174	2.13, 2.62, 5.19, 5.19, 4.66, 2.81, 5.39, 2.13, 4.85	-5.2
6HIX+CPX	TYR A:50, ARG A:52, HIS A:214, ILE A:42	2.67, 7.80, 3.17, 5.1	-5.2
6MIT+PAM	TYR A:47, THR A:45, PHE A:46, VAL A:18	2.05, 4.42, 2.73, 5.22	-8.0
6MIT+EIA	PRO A:37, GLU A:163, ASP A:162, TYR A:47, THR A:45, LYS A:11, VAL A:19, TYR A:13, VAL A:18	2.89, 3.35, 4.97, 2.84, 2.70, 4.56, 5.22, 4.56, 3.93	-8.4
6MIT+CPX	HIS A:195, ASN B:196, ASP B:194, ALA B:166, GLU B:163	4.95, 2.12, 2.70, 3.13, 4.47, 3.14	-7.1
1RG7+PAM	ARG A: 52, PHE A:31, ILE A:50, ASN A:18	2.32, 3.72, 4.73, 4.74, 2.70	-8.70
1RG7+CPX	LYS A:32, ARG A:52, LEU A:28, ILE A:50	2.36, 2.31, 3.82, 5.40	-7.10
7O4C+PAM	LYS A:649	5.48	-5.80
7O4C+CPX	PRO A:646, LYS A:649, SER A:621, GLU A:632	4.66, 2.95, 2.45, 3.22	-5.10
8FFK+PAM	LYS B: 292, SER B:79	2.30, 2.40	-8.4
8FFK+CPX	LYS A:131, LYS B:110, ASN B:70, GLY A:173, ASP A:174: 4.48, GLN B: 67, SER A: 167, LEU B: 113	3.64, 5.27, 3.36, 4.20, 4.48, 3.31, 2.98, 4.97	-8.1

Table 9: Molecular interactions involved in the selected complexes and the amino acids present.

Interaction	Hydrogen bond	Carbon-Hydrogen bond	Alkyl	Pi-Alkyl	Pi-anion	Pi-sigma	Amide-Pi stacked	Halo-bond
6MIT+EIA	PRO37 ASP162 TYR47 THR45	GLU163	LYS11 VAL19 VAL18	TYR13				
1RG7+CIP	LYS32 ARG52			ILE50		LEU28		
1RG7+PAM	ARG52 ASN18		PHE31	ILE50		PHE31		
7O4C+PAM	LYS649							
8FFK+PAM	LYS110 ASN70 GLN67 SER167	LYS131	LEU113		ASP174		GLY173	ASN70

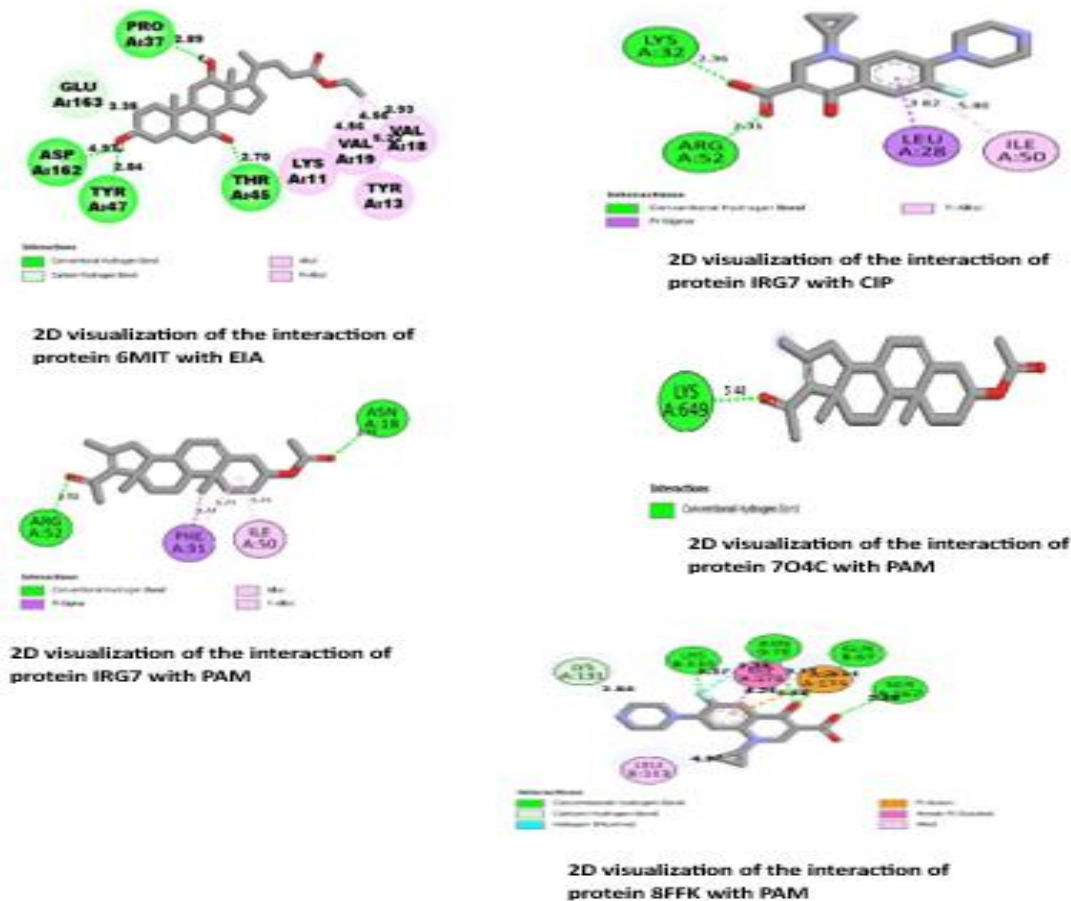


Figure 3: Molecular interactions of various proteins and ligands.

Table 10: ADMET properties of the three modelled compounds (PAM and EIA).

Compounds	PAM	EIA	Acceptable Limits
Physicochemical Properties			
Formula	C ₂₄ H ₃₄ O ₃	C ₂₆ H ₄₄ O ₅	-
Molecular weight g/mol	370	436	< 500 g/mol
Fraction Csp3	0.73	0.95	-
Num. rotatable bonds	3	6	< 10
Num. H-bond acceptors	3	5	< 10
Num. H-bond donors	0	4	< 5
Molar Refractivity	99.43	106.78	-
Topological polar surface area (TPSA)	43.37 Å ²	97.99 Å ²	< 140 Å ²
Lipophilicity			
Log Po/w (iLOGP)	3.21	0.00	-2 to 6
Log Po/w (XLOGP3)	4.57	3.20	-2 to 6
Log Po/w (WLOGP)	4.62	3.03	-2 to 6
Log Po/w (MLOGP)	4.01	2.62	-2 to 6
Log Po/w (SILICOS-IT)	4.13	2.06	-2 to 6
Consensus Log Po/w	4.11	2.18	-2 to 6
Water solubility			
Log S (ESOL)	-4.64	-3.84	> -4
Solubility	7.77e-03 mg/ml; 2.27e-05 mol/l	5.57e-02 mg/ml; 1.45e-04 mol/l	
Class	Moderately soluble	Soluble	
Log S (Ali)	-5.20	-4.93	> -4
Solubility	2.14e-03 mg/ml; 6.25e-06 mol/l	4.51e-03 mg/ml; 1.18e-05 mol/l	
Class	Moderately soluble	Moderately soluble	

Log S (SILICOS-IT)	-3.93	-1.47	> -4
Solubility	3.99e-02 mg/ml; 1.16e-04 mol/l	1.30e+01 mg/ml; 3.39e-02 mol/l	
Class	Soluble	Soluble	
Pharmacokinetics			
Gastrointestinal absorption	High	High	Depends on therapeutic target and formulation
Blood-Brain Barrier	Yes	No	Typically, low permeability for CNS drugs
p-glycoprotein substrate	No	Yes	Depends on therapeutic target and formulation
Cytochrome P450 1A2 inhibitor	No	No	Depends on therapeutic target and metabolism
Cytochrome P450 2C19 inhibitor	No	No	Depends on therapeutic target and metabolism
Cytochrome P450 2C9 inhibitor	Yes	No	Depends on therapeutic target and metabolism
Cytochrome P450 2D6 inhibitor	No	No	Depends on therapeutic target and metabolism
Cytochrome P450 3A4 inhibitor	No	No	Depends on therapeutic target and metabolism
Log Kp (skin permeation)	-5.14 cm/s	-6.37 cm/s	Depends on the intended route of administration
Drug-likeness			
Lipinski (Pfizer) filter	Yes; 0 violation	Yes; 0 violation	No more than 1 violation
Ghose filter	Yes	Yes	No more than 1 violation
Veber (GSK) filter	Yes	Yes	No more than 1 violation
Egan (Pharmacia) filter	Yes	Yes	No more than 1 violation
Muegge (Bayer) filter	Yes	Yes	No more than 1 violation
Abbott Bioavailability score	0.55	0.56	>0.5
Medicinal Chemistry			
Pan assay interference structure (PAINS)	0 alert	0 alert	No specific limits
Brenk structural alert	2 alerts: aldehyde, isolated alkene	0 alert	No specific limits
Lead-likeness	No; 1 violation: XLOGP3>3.5	No; 1 violation: MW>350	-
Synthetic accessibility score	5.17	4.91	1-10

DISCUSSION

The antibacterial activities of fractions of *A. cordifolia* leaf ethanol extract *against* the test bacterial isolates, showed that *n*-hexane fraction exhibited low antibacterial activity against the test bacterial isolates. This result is somewhat similar to previous report by Mogana et al. (2020), where the authors used *Canarium pateninervium* Miq. Also, this study is in agreement with previous report by George et al. (2010). The low antibacterial activity observed for *n*-hexane fraction is suggestive of the fact that either the bioactive compounds of *A. cordifolia* leaf may not be lipophilic or could not diffuse adequately through the agar plate (Ekundayo et al., 2020). The dichloromethane (DCM) fraction showed good antibacterial activities against the test bacterial isolates. Comparatively, DCM fraction exhibited a better activity than *n*-hexane fraction. The DCM fraction showed good activity against the test bacterial isolates. Antibacterial activity of medicinal plants have been widely reported and is often due to the presence of several phytoconstituents (Mbah et al., 2012). The

butanol and ethyl acetate fractions, showed remarkable antibacterial activities against all the test bacterial isolates. Comparatively, the butanol fraction showed better activity and was more active against Gram-negative bacteria while ethyl-acetate showed better activity against Gram-positive bacteria than Gram-negative bacteria, indicating that these fractions have broad spectrum of antibacterial activity as such, could be used to treat infections caused by members of Enterobacteriaceae, *S. aureus* and *B. thuringiensis* (Adeshina et al., 2012). The butanol and ethyl-acetate fractions exerted high inhibition against the various test bacterial isolates at the highest concentration with values ranging from 15.5±0.5 mm for *B. thuringiensis* to 26.0±1.0 mm for *K. pneumoniae* and 15.0±0.0 mm for *E. cloacae* to 25.0±1.0 mm for *K. pneumoniae* respectively. Similar activity was also reported by Mohammed and Ado, (2022) using ethyl-acetate fraction. As clearly shown in the present study, the butanol and ethyl-acetate fractions possess inhibitory properties at varying degrees. The higher inhibitory efficacy of butanol and ethyl-

acetate fractions might be attributed to the higher proportion of some of these secondary metabolites namely phenol, alkaloids, flavonoids and fatty acids in these fractions. From the results of this study, Gram negative bacteria showed more sensitivity to the butanol fraction of *A. cordifolia* leaf ethanol extract than Gram positive bacteria, while ethyl-acetate fraction demonstrated higher activity against Gram-positive bacteria than Gram-negative bacteria. The differences in the sensitivity of the test bacterial isolates to the fractions could be attributable to the breakdown of lipopolysaccharide (LPS) of Gram-negative bacteria, thus allowing the permeation of the bioactive phytoconstituents of the fractions (Mohammed and Ado, 2022). Similarly, high efficacy of ethyl-acetate fraction against Gram-positive bacteria could be attributed to the inhibition of the synthesis of wall teichoic acid predominantly present in Gram positive bacteria, by the bioactive compounds. Pasquina *et al.* (2013), opined that wall teichoic acid could be a new antibacterial agent target, as such inhibiting its biosynthesis will resensitize methicillin resistance *S. aureus* (MRSA) to β -lactam drugs. The aqueous fraction exerted the highest inhibition against *E. coli* with inhibition zone value of 16.0 ± 1.0 mm. Also, the aqueous fraction had little activity against *P. mirabilis* with inhibition zone diameter of 11.0 ± 0.0 mm. This result is expected because the active compounds are non-polar in nature, as such the compound's solubility may be low or absent in the aqueous medium (Adoukpe *et al.*, 2022). The result of this study agrees with the previous study by Kebede and Shibeshi, (2022) as it was effective against *E. coli*, however, there was no efficacy against *K. pneumoniae* and *S. aureus* using *Ricinus communis*.

Equally, the MIC and MBC values of butanol fraction varied and ranged from 31.25 to 125 mg/mL. Gram-negative bacteria were more sensitive to the fraction with lower MICs and MBCs than the Gram-positive bacteria, indicating good inhibitory activities against Gram-negative bacteria.

The GC-MS analysis of butanol and ethyl-acetate fractions of *A. cordifolia* leaf ethanol extract revealed the presence of 15 and 13 compounds respectively. Some of the identified compounds have been previously reported to possess therapeutic properties. For instance, hexadecenoic acid-1,1- dimethyl ethyl ester, 9,12-Octadecadienoic acid, Octadecanoic acid, γ -Sitosterol, linoleic acid and oleic acid possess antioxidant, anti-inflammatory and anti-cancer properties (Okereke *et al.*, 2017; Okagu *et al.*, 2018). The presence of these bioactive compounds give credence to the use of the plant for treatment and prevention of various diseases by traditional practitioners. However, isolation of individual phytoconstituents for the production of novel drugs and subjecting them to biological and pharmacological activities will likely give better results.

The molecular docking result revealed that hydrogen bonding is the prevailing force controlling the interactions between the docked compounds and the protein targets (Umar *et al.*, 2020). Comparatively, the strong affinities of the ligands to the protein targets resulted in highly negative binding affinities, which indicate that the ligands bind firmly with the protein targets (with varying amino acid residues) than the standard drugs, ciprofloxacin. Hence, the ligands (PAM and EIA) could be used as novel inhibitors of the specific proteins expressed (Lee *et al.*, 2008 and Hasan *et al.*, 2021); as evident in the molecular docking results. The bond lengths between atoms in a molecule or between molecules play a crucial role to determine interaction strength. As such, in molecular docking, shorter bond lengths indicate stronger interactions (Gibbs *et al.*, 2013). The shorter bond lengths observed with their respective interacting amino acid residues suggests strong and stable interactions with the different protein targets, thus, contributing to their binding energies (Gibbs *et al.*, 2013).

The molecular docking results lay a promising foundation and corroborate the potential of the ligands (PAM and EIA) as novel inhibitors of the protein targets from *B. thuringiensis*, *E. coli*, *S. aureus*, *K. pneumoniae*, *P. mirabilis* and *E. cloacae*, which is evident in the *in vitro* reports of this study. There is limited literature relating to interactions of these protein targets and the ligands, as such, comparison with previous studies is challenging.

Furthermore, the ligands, PAM and EIA were evaluated for their drug-likeness and pharmacokinetics ADMET properties. From the result of the study, the ligands met all the drug-likeness filters (Lipinski, Ghose, Veber, Muegge and Egan) with no violation, which is indicative of the ligands' adherence to the principles that guide the design of successful drug candidates (Dahiru *et al.*, 2024). The ligands exhibited high gastrointestinal absorption properties with moderate solubility, though PAM is not predicted to be p-glycoprotein substrate, but EIA is a p-glycoprotein substrate. The p-glycoproteins act as barrier, detoxifying the cell by extruding toxins and foreign compounds from the cell (Pires *et al.*, 2015). Also, the ligands were predicted to be skin permeable, because they exceeded the threshold value of > -2.5 cm/s (Dahiru *et al.*, 2024). Furthermore, the oral bioavailability showed that the ligands demonstrated good potential bioavailability, which is critical for the ligands effectiveness when administered (Umar *et al.*, 2020 and Dahiru *et al.*, 2024). Summarily, all the ligands exhibited good pharmacokinetics properties and as such could be potential novel inhibitors of the specific proteins to curb the menace of AMR.

CONCLUSION

The pharmacological and therapeutic activities of *A. cordifolia* leaf is evident in the wide reports and the identified bioactive phytoconstituents. The molecular

docking revealed high binding affinity between the ligands and the protein targets. Also, the ADMET properties showed that the compounds; PAM, EIA could be novel antibacterial agent that could be used in treating bacterial infections. Therefore, further *in vivo* studies on the compounds are recommended to ascertain its efficacy and safety in the treatment and prevention of human bacterial infections.

ACKNOWLEDGEMENT

We acknowledge and thank TETFund for sponsoring this research through Institution Based Research (IBR). The authors also acknowledge the University of Uyo, Uyo for using their facilities.

REFERENCES

1. Abubakar, A. R. and Haque, M. Preparation of Medicinal Plants: Basic Extraction and Fractionation Procedures for Experimental Purposes. *Journal of Pharmacy and BioAllied Sciences*, 2020; 12(1): 1–12. <https://doi.org/10.4103/jpbs.JPBS>
2. Addis, T., Mekonnen, Y., Ayenew, Z., Fentaw, S. and Biazin, H. Bacterial uropathogens and burden of antimicrobial resistance pattern in urine specimens referred to Ethiopian Public Health Institute. *PLoS ONE*, 2021; 16(11): e0259602. <https://doi.org/10.1371/journal.pone.0259602>.
3. Adeshina, G. O., Kunle, O. F., Onaolapo, J. A., Ehinmidu, J. O. and Odama, L. E. Antimicrobial Activity of the Aqueous and Ethyl Acetate Sub-Fractions of *Alchornea cordifolia* Leaf. *European Journal of Medicinal Plants*, 2012; 2(1): 31–41. <https://doi.org/10.9734/ejmp/2012/917>
4. Adoukpe, F., Ayena, A. C., Aholoukpe, V., Dougnon, V., Klotoe, J.-R., Medehouenou, M. and Baba-Moussa, L. Use of the leaves of *Alchornea cordifolia* (Schumach. & Thonn.) Müll (Euphorbiaceae) and prospects for treatment of infections due to multidrug-resistant bacteria. *Bulletin of the National Research Centre*, 2022; 46(132): 1–7. <https://doi.org/10.1186/s42269-022-00821-0>
5. Ahmed, N., Khalid, H., Mushtaq, M., Basha, S., Rabaan, A. A., Garout, M., Halwani, M. A., Mutair, A., Alhumaid, S. and Alawi, Z. The molecular characterization of virulence determinants and antibiotic resistance patterns in human bacterial uropathogens. *Antibiotics*, 2022; 11: 516. <https://doi.org/10.3390/antibiotics11040516>.
6. Asimole, C., Okolo, C., Okoye, F., Okoye, N. and Okoye, E. Herbal gel of *Alchornea cordifolia* polyphenols-rich fractions displayed promising antimicrobial and wound healing activities. *Journal of Current Biomedical Research*, 2022; 2(6): 568–586. <https://doi.org/10.54117/jcbr.v2i6.1>
7. Chaudhary, M. and Tyagi, K. A review on molecular docking and its application. *International Journal of Advance Research*, 2024; 12(03): 1141–1153. <http://dx.doi.org/10.21474/IJAR01/18505>.
8. Chikowe, I., Bwaila, K. D., Ugbaja, S. C. and Abouzie, A. S. GC–MS analysis, molecular docking, and pharmacokinetic studies of *Multidentia crassa* extracts' compounds for analgesic and anti-inflammatory activities in dentistry. *Scientific Reports*, 2024; 14: 1876. <https://doi.org/10.1038/s41598-023-47737-x>.
9. Dahiru, M. M., Abaka, A. M. and Ya, I. Antibacterial Potential of *Ximenia americana* L. Olacaceae: Molecular Docking, Molecular Dynamics, and ADMET Prediction. *Journal of Pharmacy*, 2024; 4(1): 51–67. <https://doi.org/10.31436/jop.v4i1.252>
10. Daina, A., Michielin, O. and Zoete, V. SwissADME: a free web tool to evaluate pharmacokinetics, drug-likeness and medicinal chemistry friendliness of small molecules. *Scientific Reports*, 2017; 7(1): 42717.
11. Dandekar, R., Fegade, B. and Vh, B. GC-MS analysis of phytoconstituents in alcohol extract of *Epiphyllum oxypetalum* leaves. *Journal of Pharmacognosy and Phytochemistry Materials*, 2015; 4(1): 149–154.
12. Djimeli, M. N., Fodouop, S. P. C., Njateng, G. S. S., Fokunang, C., Tala, D. S., Kengni, F., & Gatsing, D. Antibacterial activities and toxicological study of the aqueous extract from leaves of *Alchornea cordifolia* (Euphorbiaceae). *BMC Complementary and Alternative Medicine*, 2017; 17(1): 1–10. <https://doi.org/10.1186/s12906-017-1854-5>
13. Ebenyi, L., Nwakaeze, A., Moses, I., Iroha, I., Uzoeto, J., Ugochukwu, J. I., Eddison, I. O. and Okamkpa, C. J. Antibacterial activity of *Alchornea cordifolia* leaves found in Ebonyi state, Nigeria. *International Journal of Advances in Pharmacy, Biology and Chemistry*, 2017; 6(1): 46–51.
14. Effen, K. E., Kouakou-Siransy, G., Irie-Nguessan, G., Sawadogo, R. W., Dally, I. L., Kamenan, A. B., Kouakou, L. S. and Kablan-Brou, J. Acute Toxicity and Antipyretic Activities of a Methanolic Extract of *Alchornea cordifolia* Leaves. *Pharmacology & Pharmacy*, 2013; 04(07): 1–6. <https://doi.org/10.4236/pp.2013.47a2001>
15. Ekpiken, E. S., Ekong, U. S., Thomas, P. S. and Agbiji, N. N. Antibacterial Activity of Extracts of *Alchornea cordifolia* Leaf Against Selected Uropathogens. *World Journal of Pharmacy and Pharmaceutical Sciences*, 2024; 13(2): 765–781. <https://doi.org/10.20959/wjpps20242-26512>
16. Ekundayo, E. O., Kalu, U. O. and Enya, E. *In-vitro* Inhibitory Activity of Extracts of Some Medicinal Plants against *Mycobacterium smegmatis*. *Nigerian Journal of Microbiology*, 2020; 34(1): 5044–5052.
17. França, L. T. C., Carrilho, E. and Kist, T. B. L. A review of DNA sequencing techniques. *Quarterly Reviews of Biophysics*, 2002; 35(2): 169–200. <https://doi.org/10.1017/S0033583502003797>
18. George, N. J., Obot, I. B., Ikot, A. N., Akpan, A. E. and Obi-Egbedi, N. O. Phytochemical and antimicrobial properties of leaves of *Alchornea*

- cordifolia*. *E-Journal of Chemistry*, 2010; 7(3): 1071–1079. <https://doi.org/10.1155/2010/784095>
19. Gibbs, G. V., Ross, N. L., Cox, D. F., Rosso, K. M., Iversen, B. B. and Spackman, M. A. Pauling bond strength, bond length and electron density distribution. *Physics and Chemistry of Minerals*, 2013; 41(1): 1–12. <https://doi.org/10.1007/s00269-013-0619-z>
 20. Giwa, F. J., Ige, O. T., Haruna, D. M., Yaqub, Y., Lamido, T. Z. and Usman, S. Y. Extended-spectrum beta-lactamase production and antimicrobial susceptibility pattern of uropathogens in a tertiary hospital in Northwestern Nigeria. *Annals of Tropical Pathology*, 2018; 9: 11-6.
 21. Gonelimali, F. D., Lin, J., Miao, W., Xuan, J., Charles, F., Chen, M. and Hatab, S. R. Antimicrobial properties and mechanism of action of some plant extracts against food pathogens and spoilage microorganisms. *Frontiers in Microbiology*, 2018; 9(JUL): 1–9. <https://doi.org/10.3389/fmicb.2018.01639>
 22. Hartley, M. and Bennett, B. Heterologous expression and purification of *Vibrio proteolyticus* (*Aeromonas proteolytica*) aminopeptidase: a rapid protocol. *Protein expression and purification*, 2009; 66(1): 91-101.
 23. Hasan, T. H., Alasedi, K. and Aljanaby, A. *Proteus mirabilis* Virulence Factors: Review. *International Journal of Pharmaceutical Research*, 2021; 13(1): 2145–2149. <https://doi.org/10.31838/ijpr/2021.13.01.169>
 24. Ilusanya, O. A. F., Odunbaku, O. A., Adesetan, T. O. and Amosun, O. T. Antimicrobial Activity of Fruit Extracts of *Xylopiya aethiopyca* and its Combination With Antibiotics Against Clinical Bacterial Pathogens. *Journal of Biology, Agriculture and Healthcare.*, 2012; 2(9): 1–43.
 25. Jiang, W., Ubhayasekera, W., Pearson, M. M. and Knight, S. D. Structures of two fimbrial adhesins, AtfE and UcaD, from the uropathogen *Proteus mirabilis*. *Acta Crystallographica*, 2018; 74(11): 1053-1062.
 26. Kebede, B. and Shibeshi, W. In vitro antibacterial and antifungal activities of extracts and fractions of leaves of *Ricinus communis* Linn against selected pathogens. *Veterinary Medicine and Science*, 2022; 8(4): 1802–1815. <https://doi.org/10.1002/vms3.772>
 27. Kourkouta, L., Kotsiftopoulos, C. H., Papageorgiou, M., Iliadis, C. H., & Monios, A. The rational use of antibiotics medicine. *Journal of Healthcare Communications*, 2017; 2(4). DOI: 10.4172/2472-1654.100076.
 28. Lee, K. S., Bumbaca, D., Kosman, J., Setlow, P. and Jedrzejewski, M. J. Structure of a protein-DNA complex essential for DNA protection in spores of *Bacillus* species. *Proceedings of the National Academy of Sciences of the United States of America*, 2008; 105(8): 2806–2811. <https://doi.org/10.1073/pnas.0708244105>
 29. Maduabuchi, E. K. and Tobechukwu, O. P. Advanced phytochemistry and chemo-metric profiling of the bioactive medicinal components of n-hexane seed extract of *Xylopiya aethiopyca* using FTIR and GC-MS techniques. *GSC Biological and Pharmaceutical Sciences*, 2023; 22(01): 247–256. <https://doi.org/10.30574/gscbps.2023.22.1.0031>.
 30. Martínez-Caballero, S., Mahasanen, K. V., Kim, C., Molina, R., Feltzer, R., Lee, M. and Hermoso, J. A. Integrative structural biology of the penicillin-binding protein-1 from *Staphylococcus aureus*, an essential component of the divisome machinery. *Computational and Structural Biotechnology Journal*, 2023; 19: 5392-5405.
 31. Mbah, J. A., Ngemenya, M. N., Abawah, A. L., Babiaka, S. B., Nubed, L. N., Nyongbela, K. D., Lemuh, N. D. and Efange, S. M. N. Bioassay-guided discovery of antibacterial agents: In vitro screening of *Peperomia vulcanica*, *Peperomia fernandopoioana* and *Scleria striatinux*. *Annals of Clinical Microbiology and Antimicrobials*, 2012; 11: 1–10. <https://doi.org/10.1186/1476-0711-11-10>
 32. Mir, W. R., Bhat, B. A., Rather, M. A., Muzamil, S., Almilaibary, A., Alkhanani, M. and Mir, M. A. Molecular docking analysis and evaluation of the antimicrobial properties of the constituents of *Geranium wallichianum* D. Don ex Sweet from Kashmir Himalaya. *Scientific Reports*, 2022; 12: 12547. <https://doi.org/10.1038/s41598-022-16102-9>.
 33. Mogana, R., Adhikari, A., Tzar, M. N., Ramliza, R. and Wiart, C. Antibacterial activities of the extracts, fractions and isolated compounds from *Canarium patentinervium* Miq. against bacterial clinical isolates. *BMC Complementary Medicine and Therapies*, 2020; 20(55): 1–11.
 34. Mohammed, A. and Ado, B. K. Phytochemical and Antibacterial Study of Ethanol and Ethyl acetate Extracts from Leaves of *Alchornea cordifolia* Against Isolates from Infected Wounds. *Equity Journal of Science and Technology*, 2021; 8(1): 70–73. <https://doi.org/10.4314/equijost.v8i1.11>
 35. Nain, V. K., Khurana, G. S., Singh, S., Vashitha, A., Sangeeta, A. Singh, N. and Diwan, P. Antibiotic resistance pattern in bacterial isolates obtained from different water samples of Delhi Region. *DU Journal of Undergraduate Research and Innovation*, 2015; 1(3): 219-227.
 36. Nyandjou, Y. M. C. *Isolation, characterization and antibiogram of some enteric pathogenic bacteria from waste dumps in Zaria metropolis, Nigeria* (PhD thesis). Ahmadu Bello University, Zaria, 2017; 242.
 37. Okagu, I. U., Ngwu, U. E. and Odenigbo, C. J. Bioactive Constituents of Methanol Extract of *Xylopiya aethiopyca* (UDA) Fruits from Nsukka, Enugu State, Nigeria. *Open Access Library Journal*, 2018; 5(e4230): 1–11. <https://doi.org/10.4236/oalib.1104230>
 38. Okereke, S. C., Arunsi, U. O. and Nosiri, C. I. GC-MS/FT-IR screening of *Xylopiya aethiopyca* (Dunal) A. Rich Fruit. *African Journal of Biochemistry*

- Research*, 2017; 11(3): 12–17. <https://doi.org/10.5897/AJBR2016.0916>
39. Owens, T. W., Taylor, R. J., Pahil, K. S., Bertani, B. R., Ruiz, N., Kruse, A. C. and Kahne, D. Structural basis of unidirectional export of lipopolysaccharide to the cell surface. *Nature*, 2019; 567(7749): 550-553.
40. Pasquina, L. W., Santa Maria, J. P. and Walker, S. Teichoic acid biosynthesis as an antibiotic target. *Current Opinion in Microbiology*, 2013; 16(5): 531–537. <https://doi.org/10.1016/j.mib.2013.06.014>
41. Pires, D. E. V, Blundell, T. L. and Ascher, D. B. pkCSM: Predicting Small-Molecule Pharmacokinetic and Toxicity Properties Using Graph-Based Signatures. *Journal of Medicinal Chemistry*, 2015; 58: 4066–4072. <https://doi.org/10.1021/acs.jmedchem.5b00104>
42. Sawaya, M. R. and Kraut, J. Loop and subdomain movements in the mechanism of *Escherichia coli* dihydrofolate reductase: crystallographic evidence. *Biochemistry*, 1997; 36(3): 586-603.
43. Sharma, S., Kaur, N., Malhotra, S., Madan, P., Ahmad, W. and Hans, C. Serotyping and antimicrobial susceptibility pattern of *Escherichia coli* isolates from urinary tract infections in paediatric population in a tertiary care hospital. *Journal of Pathogens*, 2016; 1-4. <http://dx.doi.org/10.1155/2016/2548517>.
44. Sinan, K. I., Ak, G., Etienne, O. K., Jekó, J., Cziáky, Z., Gupcsó, K., Rodrigues, M. J., Custodio, L., Mahomoodally, M. F., Sharmeen, J. B., Brunetti, L., Leone, S., Recinella, L., Chiavaroli, A., Orlando, G., Menghini, L., Tacchini, M., Ferrante, C. and Zengin, G. Deeper insights on alchornea cordifolia (Schumach. & thonn.) müll. extracts: Chemical profiles, biological abilities, network analysis and molecular docking. *Biomolecules*, 2021; 11(2): 1–17. <https://doi.org/10.3390/biom11020219>
45. Singh, S. P., Qureshi, A. and Hassan, W. Mechanisms of Action by Antimicrobial Agents: A Review. *McGill Journal of Medicine*, 2021; 4(19): 1-10.
46. Teferi, S., Sahlemariam, Z., Mekonnen, M., Tamrat, R., Bekana, T., Adisu, Y. and Darge, T. Uropathogenic bacterial profile and antibiotic susceptibility pattern of isolates among gynecological cases admitted to Jimma Medical Center, South West Ethiopia. *Scientific Reports*, 2023; 13: 7078. <https://doi.org/10.1038/s41598-023-34048-4>.
47. Udoh, D. I., Ekong, U. S., Etang, B. B. and Udo, N. A. E. Qualitative assessment of *Uvaria chamae* (bush banana) crude extracts against wound isolated strains of *Pseudomonas aeruginosa* and *Proteus mirabilis* alongside resistance and plasmid profiles determination of the isolates. *African Journal of Microbiology Research*, 2019; 13(28): 520–530. <https://doi.org/10.5897/AJMR2019.9145>
48. Umar, A. B., Uzairu, A., Shallangwa, G. A. and Uba, S. In silico evaluation of some 4-(quinolin-2-yl) pyrimidin-2-amine derivatives as potent V600E-BRAF inhibitors with pharmacokinetics ADMET and drug-likeness predictions. *Future Journal of Pharmaceutical Sciences*, 2020; 6(61): 1–10. <https://doi.org/10.1186/s43094-020-00084-4>
49. Yun, K. W., Kim, D. S., Kim, W. and Lim, I. S. Molecular typing of uropathogenic *Escherichia coli* isolated from Korean children with urinary tract infection. *Korean Journal of Pediatrics*, 2014; 58(1): 20-27. <http://dx.doi.org/10.3345/kjp.2015.58.1.20>.
50. Zhang, Z., Morgan, C. E., Bonomo, R. A., and Yu, E. W. Cryo-EM structures of the *Klebsiella pneumoniae* AcrB multidrug efflux pump. *mBio*, 2023; 14(3): e00659-23.
51. Zhou, G., Shi, Q-S., Huang, X-M. and Xie, X-B. The three bacterial lines of defense against antimicrobial agents. *International Journal of Molecular Sciences*, 2015; 16: 21711-21733. DOI:10.3390/ijms160921711.